Environmental Research 299 (2026) 124376

Contents lists available at ScienceDirect

Environmental Research

journal homepage: www.elsevier.com/locate/envres

Satellite-based assessment of mining-related sediment influence on water quality in an extractive river basin☆

Vincent Adjei [a], Lawson Mensah [a], Alex Owusu Amoakoh [b,c,*], Mary Antwi [d], Gideon Nkrumah [a], Isaac Stanisluv Essah [e], Frederick Gyan [a], Vera Aseye Edor [a], Godfred Adu Boateng [f]

[a] Department of Environmental Science, College of Science, Kwame Nkrumah University of Science and Technology, Kumasi, AR, Ghana
[b] Liverpool Research Institute for Climate and Sustainability (LiRICS), Liverpool John Mores University, Byrom Street, Liverpool, L3 3AF, United Kingdom
[c] Natural Capital Hub, School of Biological and Environmental Sciences, Faculty of Science, Liverpool John Moores University, Liverpool, United Kingdom
[d] Department of Environmental Management, School of Natural Resources, University of Energy and Natural Resources, Sunyani, BA, Ghana
[e] Department of Wildlife and Range Management, Faculty of Renewable Natural Resources, College of Agriculture and Natural Resources, Kwame Nkrumah University of Science and Technology, Kumasi, AR, Ghana
[f] Department of Geography and Regional Planning, University of Cape Coast, Cape Coast, CR, Ghana

ARTICLE INFO

Keywords:
Land-use change
Mining disturbance
Machine learning
Sediment dynamics
Sustainability assessment

ABSTRACT

Extractive activities drive land transformation in many mineralised river basins. However, linking these changes to observable and attributable water-quality outcomes remains methodologically challenging. This study applies an integrated monitoring framework to examine how multi-decadal Land-use and land-cover change (LULC) translates into spatially differentiated river water quality in the Ankobra River basin, Ghana. Using harmonised Landsat and Sentinel imagery, LULC dynamics was reconstructed for 1986, 2002, 2016, and 2025. Field-based measurements of key physico-chemical water-quality parameters were collected to support the analysis. Spatial interpolation using Ordinary Kriging and redundancy analysis was then applied to assess the extent to which land-use composition explains the observed variation in water quality. The results showed a shift from forest-dominated land cover towards agriculture, settlement, and mining-related disturbance during the study period. Bareland/Mining expanded from less than 1% of the basin in 1986 to approximately 3.7% by 2025 (>100 km^2), while combined forest cover declined overall throughout the study period. Water-quality patterns exhibited strong spatial gradients, with turbidity ranging from approximately 114 to more than 1000 NTU and total suspended solids (TSS) from around 100 to nearly 3000 mg L^{-1}. Redundancy analysis indicated that land-use composition explained approximately 47.5% of the variance in water quality, with the mining-related land cover exerting the strongest influence ($F = 13.66$, $p < 0.001$) and showing robust positive associations with turbidity and TSS. Closed forest cover displayed a significant buffering effect, while agricultural land use did not show significant association on the spatial scale examined. These findings demonstrate how integrated Earth observation and field data can move sustainability assessment beyond descriptive convergence towards diagnostic clarity. The analytical framework offers a transparent and scalable approach for prioritising regulatory attention and monitoring in extractive landscapes where environmental pressures are spatially uneven and governance capacity is constrained.

1. Introduction

Extractive activities continue to play a central role in economic development in many low- and middle-income countries, yet their environmental and social sustainability remains persistently contested. Large-scale artisanal mining operations frequently generate extensive land disturbance, alter hydrological pathways, and introduce sediments and contaminants into river systems, with consequences that extend well beyond the immediate footprint of extraction (Bebbington et al., 2018; Hilson et al., 2020; Obodai et al., 2019). In West Africa, and especially Ghana, artisinal gold mining (ASM) has been

☆ This article is part of a Special issue entitled: 'Mining, Water, and Climate: Emerging Environmental Risks' published in Environmental Research.

* Corresponding author at: Natural Capital Hub, School of Biological and Environmental Sciences, Faculty of Science, Liverpool John Moores University, Liverpool, United Kingdom.
E-mail address: a.o.amoakoh@ljmu.ac.uk (A.O. Amoakoh).

https://doi.org/10.1016/j.envres.2026.124376
Received 4 February 2026; Received in revised form 24 March 2026; Accepted 26 March 2026
Available online 27 March 2026

associated with widespread river turbidity, sediment mobilisation, and channel modification in major basins, including Pra, Offin, Ankobra, and Birim (Hilson, 2002; Kuma and Younger, 2004; Obodai et al., 2019). These impacts shape biophysical conditions, livelihoods, regulatory legitimacy, and longer-term development trajectories, particularly in regions where rivers underpin domestic water supply, agriculture, and ecosystem services. In such settings, sustainability cannot be meaningfully assessed by production metrics or formal compliance reporting alone. It requires integrated evidence that links land-use change with observable environmental outcomes within affected river basins.

Despite this need, sustainability assessment in extractive landscapes remains fragmented. Land use dynamics is commonly monitored using satellite Earth observation, while water quality is assessed through field sampling campaigns that are often spatially limited and temporally discontinuous (Allan et al., 2017). Remote sensing can document the expansion and contraction of mining, agriculture, and settlement over time; however, it does not directly indicate how such changes translate into aquatic system degradation. In contrast, water-quality measurements can identify elevated turbidity, suspended solids, or dissolved constituents, but lack the spatial context required to attribute these conditions to specific land-use pressures. As a result, regulators and planners are often left with parallel strands of evidence that are difficult to reconcile, constraining the transition from environmental diagnosis to sustainability-oriented decision-making.

Recent advances in cloud-based geospatial platforms and analytical methods offer new opportunities to address these challenges, but their application in extractive contexts remains uneven. Long-term satellite archives, including Landsat and Sentinel, now support consistent reconstruction of land-cover trajectories over several decades, while machine-learning classifiers have improved mapping reliability in heterogeneous tropical environments (e.g., Gorelick et al., 2017; Belgiu and Drăguţ, 2016; Amoakoh et al., 2024, 2021). At the same time, spatial statistical techniques enable the visualisation of basin-scale gradients in water-quality parameters derived from discrete sampling observations, allowing environmental patterns to be examined spatially (Li and Heap, 2014). What remains less well developed is the use of these tools to support explicit attribution of water-quality variation to dominant land-use pressures in mineralised river basins. In Ghana, most mining-water studies rely on point-based sampling designs that document contamination, but do not systematically integrate long-term land-cover trajectories derived from satellite archives (e.g., Obodai et al., 2019; Armah et al., 2010; Duncan et al., 2018). Therefore, while degradation is well documented, spatial attribution of river condition to specific land-use transitions remains limited. Integrated analyses consequently remain largely descriptive, demonstrating co-occurrence between land-use change and water-quality decline without providing the diagnostic evidence needed to prioritise regulatory action or inform sustainability governance.

This study applies an integrated monitoring framework to the Ankobra Basin, Ghana, linking multi-decadal LULC dynamics with spatially distributed water-quality observations in an extractive landscape. The aim is to assess how contemporary land-use composition explains spatial variation in river water quality measured within a landscape shaped by multi-decadal transformation. Specifically, the study (i) reconstructs multi-decadal LULC trajectories in a mineralised river basin using satellite Earth observation data; (ii) characterises the spatial variability of key water-quality parameters based on field measurements, supported by spatial visualisation; and (iii) evaluates the extent to which contemporary land-cover composition explains observed spatial variation in water-quality parameters, with emphasis on sediment-related indicators. In doing so, the study adopts an attribution-oriented analytical framework aimed at improving transparency and diagnostic clarity in the assessment of sustainability (Scoones, 2016; Newell, 2019; Turnhout et al., 2020).

2. Methodology

2.1. Study area

The study was conducted in the Ankobra River basin, located in southwestern Ghana, and covers approximately 2892 km^2 in Prestea–Huni Valley (PHV) and Nzema East (NE) districts of the Western Region (Fig. 1). The Ankobra river flows south before discharging into the Gulf of Guinea at Sanwoma. Prestea–Huni Valley district occupies approximately 1809 km^2 of the basin and is characterised by undulating terrain and a long history of industrial and artisanal gold mining centred around Bogoso (Opoku et al., 2017; Wiafe et al., 2022). The NE district covers approximately 1083 km^2 of the basin.

The area experiences a humid equatorial climate with bimodal rainfall ranging from approximately 1500 to 2000 mm annually (Cudjoe et al., 2023). Vegetation transitions from moist semi-deciduous forests in the northern part of the basin to secondary forests and coastal savannahs in the south, interspersed with forest reserves and extensive rubber and cocoa plantations (Obodai et al., 2019). Economic activities are dominated by agriculture, mining, forest management and fishing, resulting in sustained anthropogenic pressure on riparian zones and forest ecosystems. The basin contains multiple licensed mining concessions (Fig. 1), reflecting its role in Ghana's gold production corridor. Documented multi-decadal expansion of mining-related disturbance and forest-to-agriculture transitions in both districts creates marked spatial heterogeneity in land-use composition (e.g., Amoakoh et al., 2021, 2024; Obodai et al., 2019). These characteristics make the Ankobra basin a suitable case for examining how cumulative land-use change influences spatial variation in river water quality within an extractive landscape.

2.2. Satellite data and pre-processing

Multi-temporal satellite imagery was used to analyse the LULC dynamics at four time points that represent long-term change in the basin (Table 1). Surface reflectance products, from Landsat and Sentinel missions were accessed via the Google Earth Engine (GEE) cloud platform (Google LLC, Mountain View, California, USA), which provides consistent pre-processing and facilitates temporal compositing at basin scale (Gorelick et al., 2017). Landsat data were obtained from the United States Geological Survey (USGS) archive, including Landsat 5 Thematic Mapper (TM) imagery for 1986 and Landsat 7 Enhanced Thematic Mapper Plus (ETM+) imagery for 2002. Sentinel-2 Multispectral Instrument (MSI) imagery for 2016 and 2025 was provided by the European Space Agency (ESA). These time points were selected to capture pre-intensification, transition, and recent phases of land-use change, while ensuring sufficient cloud-free observations for reliable compositing in a persistently cloudy tropical environment. Sentinel-2 MSI imagery was used for the later time points due to its availability during the most recent period and its high revisit frequency, which improves the likelihood of obtaining cloud-free observations in humid tropical environments. To minimise atmospheric effects and data gaps, annual image composites were generated using scenes with less than 10% cloud cover. Cloud-affected pixels were removed using the GEE cloud probability masking approach, and median composites were produced to reduce residual noise. This approach ensured temporal comparability across years while maximising spatial coverage for classification.

All satellite images were harmonised to a common spatial resolution prior to classification. Sentinel-2 MSI bands were resampled at 30 m to match the native spatial resolution of the Landsat imagery. This resolution was selected to preserve comparability across the full temporal range of the analysis while avoiding artificial inflation of spatial detail in earlier years. Resampling was performed using a bilinear interpolation approach for continuous spectral bands, which minimises aliasing effects and preserves radiometric continuity relative to nearest-neighbour methods (Jensen, 2016).

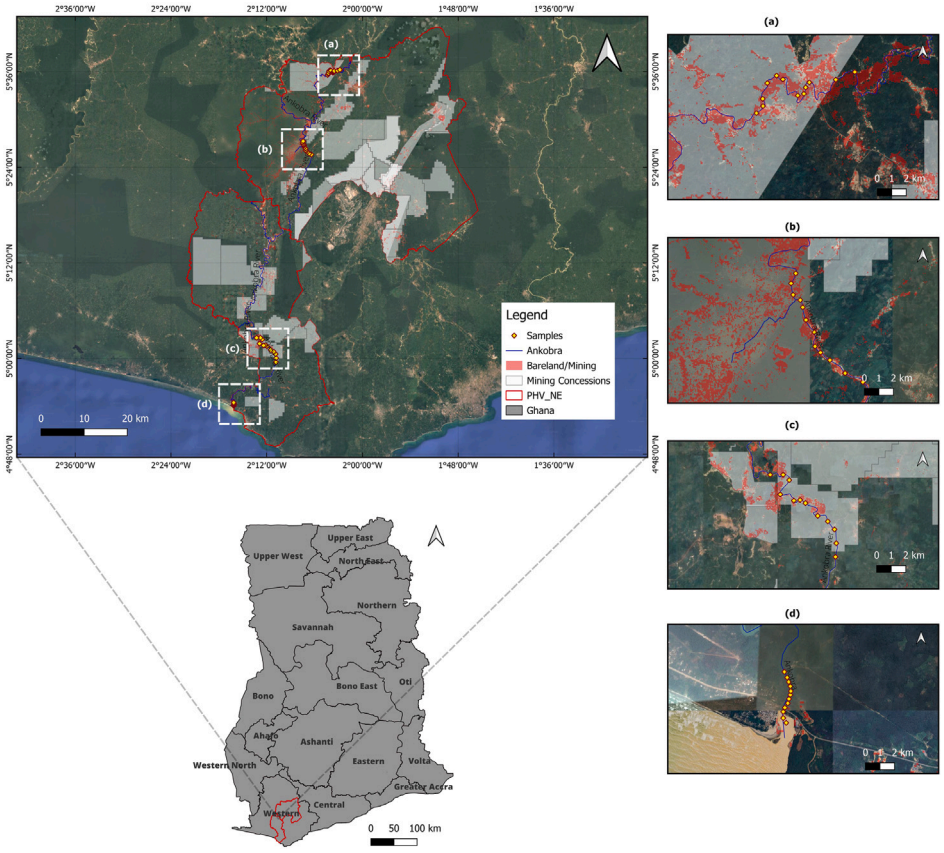

Fig. 1. Study area map of the Ankobra River Basin showing the Prestea–Huni Valley (PHV) and Nzema East (NE) districts. The map displays water-quality sampling locations, the Ankobra River network, 2025 Bareland/Mining areas derived from the land-cover classification, and licensed mining concession boundaries obtained from the Ghana Mining Repository (Minerals Commission of Ghana, 2026). Insets (a–d) provide detailed views of selected river reaches and sampling points. Basemap imagery © Google.

Table 1
Satellite imageries used for LULC analysis.

Year	Satellite	Spatial resolution (m)
1986	Landsat 5 TM	30
2002	Landsat 7 ETM+	30
2016	Sentinel-2 MSI (L1C)	10, 20, 60
2025	Sentinel-2 MSI (L2A)	10, 20, 60

2.3. Land cover classification

Supervised classification was applied to the annual composites to derive LULC maps for each study year. Standard spectral band combinations, including natural colour, false colour infrared, and shortwave infrared–near infrared composites, were used to support visual interpretation and training sample selection. A Random Forest classifier was implemented within Google Earth Engine due to its robustness to non-linear relationships and its demonstrated performance in heterogeneous tropical landscapes (Amoakoh et al., 2021).

Six LULC classes were defined based on dominant land-use characteristics and spectral similarity within the basin: water, bareland/mining, settlement, agriculture, closed forest and open forest (Table 2). Mining pits and other exposed surfaces were grouped under a single Bareland/Mining class due to their similar spectral reflectance characteristics. The class captures surface conditions associated with gold extraction, including both industrial and artisanal operations, without differentiating between mining types. Although bare ground and mining pits are functionally distinct land uses, aggregation was adopted to represent sediment-relevant exposure at 30 m resolution. Therefore, the class does not correspond directly to the formally delineated concession boundaries (see Fig. 1) and may marginally overestimate the footprint of active mining areas. Dense cocoa farms, mature rubber plantations, and intact forest were operationally classified as Closed Forest based on high canopy density, while areas of sparse vegetation, fallow land, shrubs, and young plantations were classified as Open Forest to represent low vegetation cover.

Training samples for the 2025 classification were derived from field-verified coordinates and high-resolution reference imagery. These samples were transferred to earlier years through visual interpretation of historical imagery to ensure temporal consistency in class definitions across the study period.

2.4. Post classification change analysis and accuracy assessment

Post-classification change detection was conducted to quantify transitions between LULC classes over three periods: 1986–2002, 2002–2016, and 2016–2025. Cross-tabulation matrices were generated using TerrSet 19.0.6 (Clark Labs, Clark University, USA) to calculate area changes and transition patterns, allowing the identification of dominant land-cover conversions over time. The classification accuracy was assessed using confusion matrices derived from independent validation samples.

Table 2
Description of LULC classes.

LULC class	Description
Water	Rivers and water-filled mining pits
Bareland/Mining	Mining-disturbed surfaces and exposed bare ground
Settlement	Buildings, developed areas, and impervious surfaces
Agriculture	Croplands and farmlands
Closed Forest	Dense forest and high-canopy plantations
Open Forest	Sparse vegetation, shrubs, and fallow land

Overall accuracy, precision, recall, and F1-score were computed using GEE's built-in accuracy assessment functions, following standard definitions (Allan, 2004):

$$\text{Overall Accuracy} = \frac{\text{Number of correctly classified pixels}}{\text{Total number of pixels}} \times 100 \quad (1)$$

$$\text{Precision} = \frac{TP}{TP + FP} \quad (2)$$

$$\text{Recall} = \frac{TP}{TP + FN} \quad (3)$$

$$\text{F1-score} = 2 \times \frac{\text{Precision} \times \text{Recall}}{\text{Precision} + \text{Recall}} \quad (4)$$

where *TP* (true positives) represents correctly classified pixels for a given LULC class, *FP* (false positives) represents pixels incorrectly assigned to that class, and *FN* (false negatives) represent pixels belonging to that class that were incorrectly assigned to another class.

2.5. Water-quality data collection and analysis

Water-quality sampling followed a stratified design that combined the purposive delineation of the river reaches with random sampling within each stratum. The river was divided into four reaches that represent upstream and downstream conditions, as well as the spatial distribution of dominant land-use pressures within the study area. Within each reach, water samples were collected at randomly selected locations along the river, yielding a total of 48 samples in all strata. Candidate sampling locations were generated using a random point algorithm constrained to the river polyline within each reach in ArcGIS (Esri Inc., Redlands, California, USA). Where randomly generated locations were inaccessible due to terrain or safety constraints, the nearest accessible point within a short upstream or downstream tolerance was sampled. This preserved random allocation while accommodating practical field constraints and minimising systematic accessibility bias. Sampling was conducted between January and February 2025, during the peak dry season in southwestern Ghana, reducing short-term rainfall-driven variability and facilitating clearer identification of spatial contrasts associated with near-stream land-use pressures.

In situ measurements of turbidity, pH, dissolved oxygen (DO), electrical conductivity (EC), and total dissolved solids (TDS) were obtained using a HANNA HI 9829 multiparameter probe (Hanna Instruments Inc., Woonsocket, Rhode Island, USA). For total suspended solids (TSS) analysis, water samples were collected in 500 mL high-density polyethylene bottles and transported in an icebox at temperatures below 4 °C prior to laboratory (Adusei et al., 2021). Laboratory determination of TSS was conducted using the DR3900 Spectrophotometer (Hach Company, Loveland, Colorado, USA).

Spatial patterns of the water-quality parameters were estimated using Ordinary Kriging based on euclidean distance in ArcGIS 10.8. This method was selected because it explicitly accounts for spatial autocorrelation and is suitable for datasets where sampling points are unevenly distributed or clustered (Osei et al., 2024). A spherical semivariogram model was specified within the ArcGIS Kriging tool. The interpolation assumed isotropic spatial dependence and did not explicitly model nested spatial structures, reflecting the moderate sample density and linear distribution of sampling points along the river corridor. The method estimates unknown values as a weighted linear combination of observed samples (5):

$$Z^*(x) = \sum_{i=1}^{n} \lambda_i \, Z(x_i) \quad (5)$$

where λ_i are the kriging weights and $Z(x_i)$ represents the observed values at sampled locations. The resulting interpolated surfaces were used to visualise spatial variability in water-quality conditions and to identify areas of elevated environmental pressure within the basin.

2.6. Linking land use and water quality through redundancy analysis

Redundancy analysis (RDA) was employed to examine the extent to which spatial variation in water-quality parameters could be explained by surrounding land-use composition. RDA is a constrained ordination technique that combines multiple regression with principal component analysis, allowing direct assessment of relationships between explanatory and response variables (Ma et al., 2025). For each sampling location, land-use composition was quantified as the percentage cover of each LULC class within a 250 m buffer derived from the 2025 land-cover map. The buffer was defined to represent the direct influence of the riparian and near-channel land-uses. In humid tropical systems, sediment mobilisation is strongly mediated by disturbance within immediate stream corridors, where vegetation removal and soil exposure enhance delivery to adjacent channels (Naiman and Decamps, 1997; Dosskey et al., 2010). Although sediment processes operate at broader catchment scales, the analysis was designed to capture land-use pressures proximal to sampling locations rather than to model full watershed dynamics.

The water-quality parameters measured at the same locations were standardised prior to analysis to ensure comparability. In matrix form, RDA can be expressed as a multivariate linear model of the form:

$$\mathbf{Y} = \mathbf{XB} + \mathbf{E} \quad (6)$$

where **Y** is the matrix of standardised water-quality response variables, **X** is the matrix of land-use explanatory variables, **B** is the matrix of regression coefficients, and **E** represents residual variation not explained by land use.

The RDA was implemented in R using the vegan package (version 2.7-2), with LULC classes specified as explanatory variables and water-quality parameters as response variables. Statistical significance was assessed using Monte Carlo permutation tests, enabling the evaluation of whether the observed relationships differed from those expected by chance. This provided a statistically grounded basis for assessing the extent to which the current (2025) land-use composition explains the observed spatial variation in water-quality parameters within the extractive landscape.

3. Results

3.1. LULC dynamics

LULC analysis revealed substantial spatial and temporal change in the Ankobra River basin between 1986 and 2025 (Fig. 2; Table 3). In 1986, the basin was predominantly characterised by Closed Forest and Open Forest classes, which together covered more than half of the

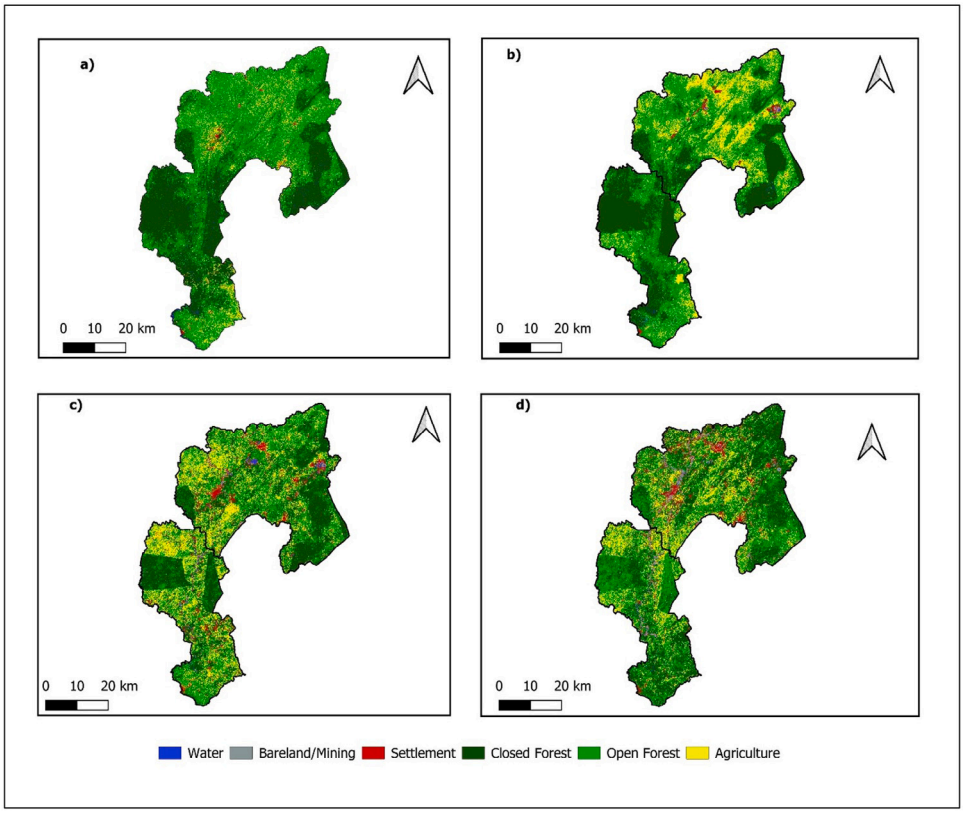

Fig. 2. Spatial distribution of LULC classes in the Ankobra River basin for (a) 1986, (b) 2002, (c) 2016, and (d) 2025.

basin area, reflecting relatively intact forest cover. Agricultural land occupied a smaller proportion of the landscape, while Bareland/Mining and Settlement each accounted for less than 5% of total land cover. Between 1986 and 2002, the most pronounced changes were associated with the expansion of agricultural land and Bareland/Mining areas, particularly within the Prestea–Huni Valley district. Agricultural land approximately doubled in extent during this period, while forest cover declined through transitions mainly from Closed Forest to Open Forest and Agriculture (Table 3, Table A.2). The expansion of Settlement remained spatially concentrated around existing urban centres and transport corridors and increased substantially between 2002 and 2016; however, its proportional contribution to total basin area remained smaller than agriculture and forest transitions.

Between 2002 and 2016, Bareland/Mining expanded sharply, increasing by more than an order of magnitude compared to 1986, exceeding 100 km^2 by 2025 (Fig. 2). This expansion coincided with continued net losses in both closed and open forest classes. Agricultural land continued to expand, although at a slower rate relative to mining-related disturbances, while Settlement growth became more spatially evident, reflecting increased urbanisation and infrastructure development. The dynamics between 2016 and 2025 continued to reflect a strong anthropogenic influence, particularly through the further expansion of bareland/mining, which increased substantially to exceed 100 km^2 by 2025 (Fig. 2). In contrast, Agricultural land declined relative to 2016 levels, while both closed forest and open forest classes exhibited moderate increases. The extent of settlement remained broadly stable during this period (Fig. 3).

3.2. Accuracy assessment of land-cover classification

Overall classification accuracy ranged from 81% to 92% during the study period (Table 4). At the class level, Water, Closed Forest, and Open Forest were generally well classified across all years, with F1-scores ranging from 0.84 to 0.94 (Table 4). Classification performance for Bareland/Mining and Settlement exhibited greater variability, particularly in earlier years, with F1-scores between 0.76 and 0.83, reflecting spectral similarity to other exposed or impervious surfaces. Classification performance for these classes improved in 2025, with F1-scores approaching 0.90, indicating improved discrimination in the higher-resolution Sentinel-2 data.

3.3. Spatial patterns of water-quality parameters

Turbidity and total suspended solids (TSS) exhibited elevated concentrations in river sections downstream of major mining areas, particularly within the Prestea–Huni Valley district (Fig. 4). Turbidity values ranged from approximately 114 to over 1000 NTU, while TSS concentrations varied between 101 and nearly 3000 mg L^{-1}, with elevated values occurring in spatially clustered segments rather than uniformly along the river network. Electrical conductivity (EC) and total dissolved solids (TDS) displayed increasing trends towards the lower reaches of the basin, especially near the coastal zone. EC values ranged from approximately 65 μS cm^{-1} upstream to over 12,000 μS cm^{-1} near the estuary, while TDS concentrations varied from below 100 mg L^{-1} in upstream sections to values exceeding 6000 mg L^{-1} in downstream reaches (Fig. 4). Dissolved oxygen (DO) concentrations showed moderate spatial variability, ranging from approximately 4.6 to 6.8 mg L^{-1}, with lower values observed in river segments adjacent to intensive land disturbance. In contrast, pH values varied within a relatively narrow range, from approximately 5.2 to 6.8, indicating generally acidic to near-neutral conditions across the basin. Summary statistics for all water-quality parameters are provided in Table 5.

3.4. Relationships between land use and water quality

The redundancy analysis (RDA) showed that land-use composition explains a substantial proportion of the observed variation in water-quality parameters. The constrained model was statistically significant

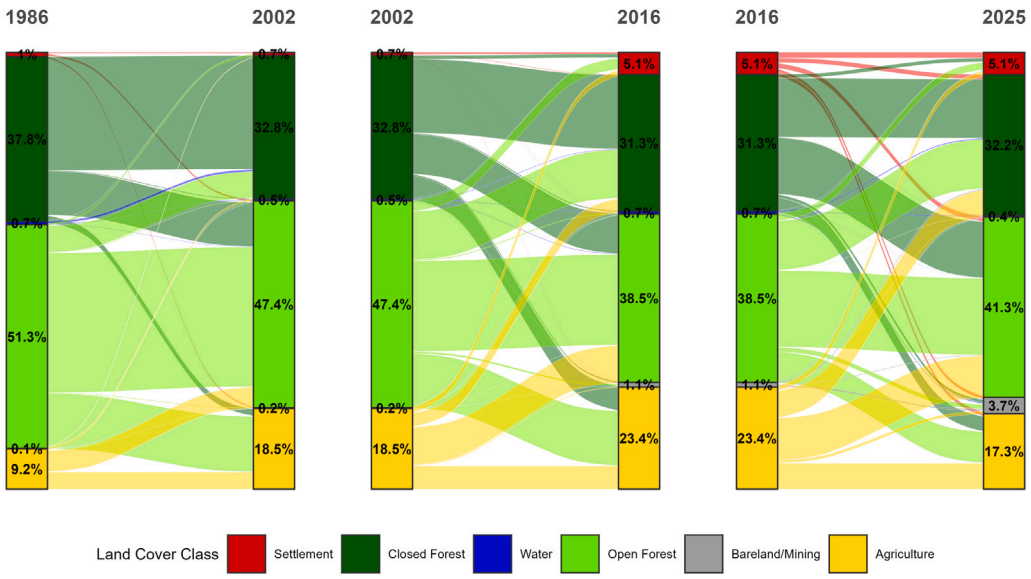

Fig. 3. LULC transition pathways in the Ankobra River basin between 1986–2002, 2002–2016, and 2016–2025, shown using Sankey diagrams. Percentages indicate the share of total basin area occupied by each class at the beginning and end of each transition period.

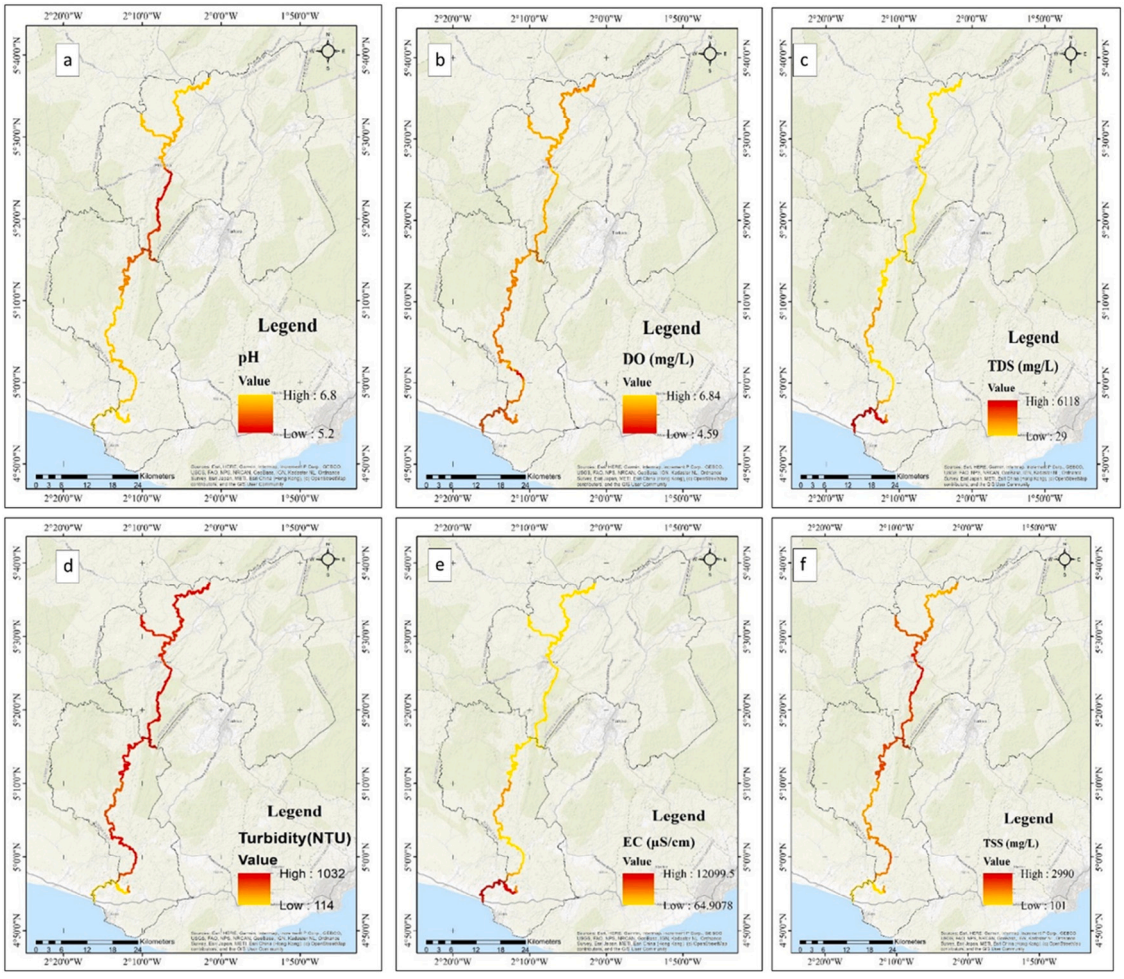

Fig. 4. Spatial distribution of interpolated water-quality parameters along the Ankobra River system: (a) pH, (b) dissolved oxygen (DO), (c) total dissolved solids (TDS), (d) turbidity, (e) electrical conductivity (EC), and (f) total suspended solids (TSS). Values represent kriged surfaces derived from field measurements, illustrating longitudinal gradients and localised zones of elevated concentrations along the river network.

Table 3
LULC area statistics for the Ankobra River basin (km^2 and %).

LULC class	1986		2002		2016		2025	
	Area (km^2)	%	Area (km^2)	%	Area (km^2)	%	Area (km^2)	%
Water	19.99	0.69	13.17	0.46	19.76	0.68	10.90	0.38
Bareland/Mining	3.07	0.11	4.96	0.17	30.46	1.05	107.96	3.73
Settlement	28.21	0.98	21.39	0.74	146.91	5.08	148.38	5.13
Closed Forest	1092.07	37.76	948.74	32.81	904.48	31.27	932.86	32.26
Open Forest	1482.34	51.26	1369.89	47.37	1114.11	38.53	1192.72	41.24
Agriculture	266.34	9.21	533.86	18.46	676.08	23.38	499.12	17.26
Total	2892.02		2892.01		2891.80		2891.94	

Table 4
LULC classification accuracy assessment across study years.

LULC class	1986			2002			2016			2025		
	Precision	Recall	F1-score	Precision	Recall	F1-score	Precision	Recall	F1-score	Precision	Recall	F1-score
Water	0.85	0.91	0.88	0.88	0.91	0.90	0.81	0.87	0.84	0.93	0.95	0.94
Bareland/Mining	0.82	0.78	0.80	0.85	0.81	0.83	0.77	0.75	0.76	0.89	0.90	0.90
Settlement	0.81	0.85	0.83	0.82	0.85	0.83	0.77	0.82	0.79	0.88	0.91	0.90
Agriculture	0.82	0.84	0.83	0.80	0.86	0.83	0.75	0.79	0.77	0.88	0.90	0.89
Closed Forest	0.90	0.85	0.88	0.89	0.89	0.89	0.87	0.84	0.85	0.92	0.93	0.93
Open Forest	0.90	0.88	0.89	0.95	0.86	0.90	0.93	0.80	0.86	0.99	0.90	0.94
Overall accuracy	85%			86%			81%			92%		

Table 5
Summary statistics of water quality parameters across selected communities.

Variable	Ankobra			Bepoh			Dominase			Prestea			Threshold
	Min	Max	Mean (SD)	Min	Max	Mean (SD)	Min	Max	Mean (SD)	Min	Max	Mean (SD)	
pH	6.62	6.79	6.74 (0.04)	6.31	6.83	6.57 (0.18)	6.34	6.65	6.53 (0.10)	5.29	6.55	5.78 (0.53)	6.5–8.5
DO ($mg\,L^{-1}$)	5.24	5.53	5.32 (0.08)	4.80	6.12	5.42 (0.39)	4.52	6.92	5.47 (0.68)	5.44	6.66	5.97 (0.46)	≥5
EC ($\mu S\,cm^{-1}$)	9933	13 250	11233.5 (946.4)	65	94	88.56 (8.93)	110	118	112.36 (2.11)	101	105	102.83 (1.72)	1000
TSS ($mg\,L^{-1}$)	72	186	133.77 (28.46)	443	978	750.11 (162.45)	1157	2294	1538.18 (298.52)	122	3054	2394.67 (1123.42)	50
TDS ($mg\,L^{-1}$)	4969	6688	5654.32 (534.24)	44	47	45.89 (1.05)	48	59	55.45 (2.66)	50	52	51.17 (0.98)	500
Turbidity (NTU)	82.3	327.0	147.65 (51.53)	954	1000	994.89 (15.33)	1000	1000	1000.0 (0.0)	338	1000	889.67 (270.26)	5

Note: Reference thresholds are derived from World Health Organization (2017) drinking-water guidelines and Ghana Standards Authority (2021). Values are used for contextual interpretation only.

(F = 6.95, $p < 0.001$), accounting for approximately 47.5% of the total variance in water quality (Fig. 5). The first canonical axis (RDA1) accounted for 44.2% of the constrained variance, capturing the dominant land-use gradient structuring water-quality patterns throughout the basin (Table 6). Fig. 5 shows a clear separation of sampling locations along gradients primarily associated with Bareland/Mining and, to a lesser extent, Settlement land use. Bareland/Mining exhibited the highest marginal contribution among the explanatory variables (F = 13.66, $p < 0.001$), showing strong positive associations with turbidity and TSS (Table 7). Sampling locations surrounded by higher proportions of mining-related land cover were consistently aligned with elevated sediment-related parameters.

Forest cover, particularly Closed Forest, was negatively associated with turbidity and TSS and exerted a statistically significant buffering influence on water quality (F = 10.30, $p < 0.001$). Open Forest and Settlement also contributed significantly to explaining water-quality variation, although their effects were weaker ($p < 0.05$), with Settlement showing modest associations with electrical conductivity (EC) and total dissolved solids (TDS). In contrast, Agricultural land cover did not exhibit a statistically significant relationship with any measured water-quality parameter on the spatial scale examined (F = 0.36, p = 0.728), indicating limited explanatory power within the present analytical framework. Monte Carlo permutation tests confirm that multiple land-use classes contribute significantly to spatial variation in water quality. Bareland/Mining exhibited the strongest marginal effect, particularly in relation to sediment-associated parameters, while forest cover exerted a contrasting buffering influence within the basin (see Table 7).

4. Discussion

4.1. Land-use transitions, dominant pressures, and sediment-driven river degradation

Long-term land-use transitions within the Ankobra River basin have resulted in a landscape characterised by sediment-dominated forms of river degradation, with mining-related disturbance emerging as the dominant pressure shaping spatial variation in water quality (Table 7). This interpretation is based on spatial relationships observed in 2025 and does not imply longitudinal causation across the full multi-decadal period.

During the study period, Bareland/Mining expanded from a negligible proportion of the basin (<1%, 3 km^2) to more than 100 km^2. This reflects a transition from a predominantly forested landscape to one increasingly characterised by exposed surfaces, hydrologically connected disturbance zones, and intensified human activity. Similar patterns have been documented in mineralised tropical basins, where mining expansion is frequently associated with disproportionate environmental impacts relative to its spatial extent (e.g., Hilson, 2002; Bebbington et al., 2018). In the Ankobra basin, this transformation provides an essential context for interpreting the magnitude and spatial structure of observed water-quality degradation.

The spatial patterns of turbidity and total suspended solids (TSS) are consistent with this land-use trajectory and indicate a strong sediment signal linked to mining disturbance. Turbidity values exceeding 1000 NTU and TSS concentrations approaching 3000 mg L^{-1} were observed in river segments downstream of intensive mining activity, particularly within the Prestea–Huni Valley district. By comparison,

Table 6
Canonical eigenvalues and variance explained by constrained axes.

Axis	Eigenvalue	Variance (%)	Cumulative (%)
RDA1	2.652	44.19	44.19
RDA2	0.114	1.90	46.09
RDA3	0.081	1.34	47.43
RDA4	0.003	0.04	47.47
RDA5	0.001	0.01	47.49
RDA6	<0.001	<0.01	<0.01

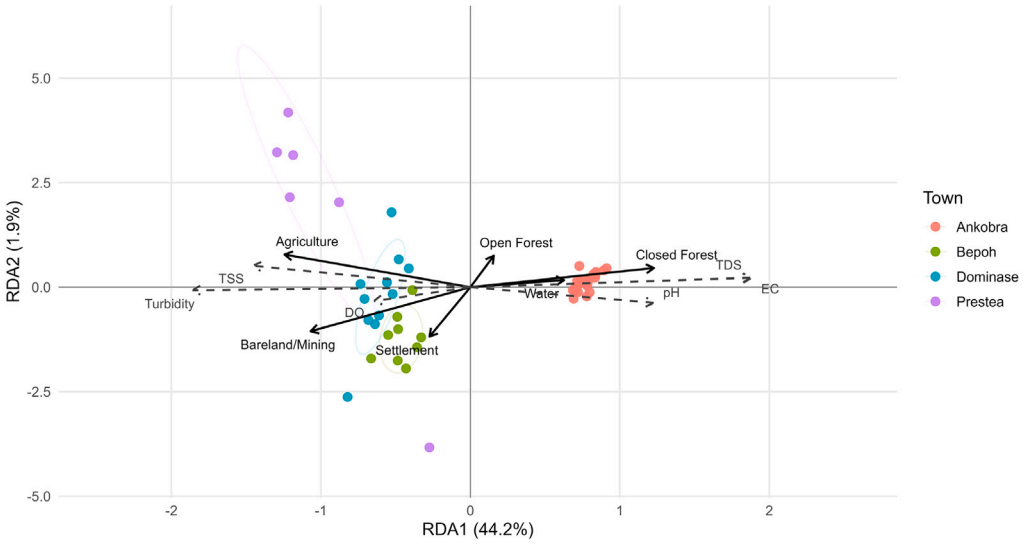

Fig. 5. RDA showing land use and land cover influence on water quality.

Table 7
Permutation test results (999 permutations) for individual land-use classes.

Land-use class	Variance	F-ratio	*p*-value
Water	0.411	5.35	0.009**
Bareland/Mining	1.050	13.66	<0.001***
Settlement	0.274	3.57	0.037*
Closed Forest	0.792	10.30	<0.001***
Open Forest	0.295	3.84	0.026*
Agriculture	0.028	0.36	0.728

* Significant at $p < 0.05$.
** Highly significant at $p < 0.01$.
*** Very highly significant at $p < 0.001$.

relatively undisturbed tropical forest rivers typically report turbidity below 2–20 NTU and suspended solids generally <5–50 mg L^{-1} (Isidore et al., 2019; Njue et al., 2021). The values observed here far exceed thresholds associated with ecological stress and reduced light penetration (commonly reported above 25–50 NTU) and exceed drinking-water guidelines, which recommend turbidity not exceeding 5 NTU (Franklin et al., 2019; EPA, 2009; Allan, 2004; Hudson-Edwards et al., 2011). Importantly, elevated sediment concentrations were not uniformly distributed across the basin but occurred in spatially clustered zones. This shows that degradation is driven by discrete disturbance hotspots rather than diffuse basin-wide pressure. Spatial concentration reflects the physical mechanisms through which mining affects fluvial systems: clearing vegetation, soil excavation, and the creation of pits and waste heaps increase sediment availability and enhance hydrological connectivity between disturbed land surfaces and adjacent channels, particularly during high-intensity rainfall events (Naiman and Decamps, 1997; Hudson-Edwards et al., 2011).

Redundancy analysis provides empirical support for linking these sediment patterns to specific land-use pressures rather than a simple spatial coincidence. The RDA model explained approximately 47.5% of the total variance in water-quality parameters, with the first canonical axis alone accounting for more than 44% of the constrained variation. Approximately 52.5% of the total variance remained unexplained. This residual variation likely reflects interacting controls beyond near-stream land-use composition. Geological heterogeneity in the Ankobra basin can influence baseline water chemistry and sediment characteristics, as variations in lithology and soil composition affect natural turbidity, dissolved constituents, and buffering capacity. In addition, hydrological conditions at the time of sampling influence sediment concentrations, which can vary markedly between baseflow and storm-driven discharge events. Although sampling was conducted during the peak dry season to reduce short-term rainfall effects, instantaneous flow variability and antecedent conditions cannot be fully controlled in cross-sectional field campaigns. These factors indicate that observed land-use associations operate within a broader hydro-geomorphic context and should be interpreted accordingly.

Bareland/Mining exerted the strongest influence on water quality ($F = 13.66$, $p < 0.001$) and showed clear positive associations with turbidity and TSS. This indicate that locations surrounded by higher proportions of mining-related land cover were characterised by elevated sediment loads. In contrast, Agricultural land cover did not exhibit statistically significant relationships with any measured water-quality parameter on the spatial scale examined. This does not suggest

that agriculture is environmentally benign, but rather highlights the scale and parameter-dependence of land-use impacts. Agricultural effects on water quality often manifest through nutrient enrichment, pesticide runoff, and fine sediment mobilisation, processes that are strongly modulated by crop type, management practices, and seasonal rainfall variability (Foley et al., 2005). In the Ankobra basin, the dominance of perennial plantation systems and the focus on sediment-sensitive physico-chemical parameters likely reduce the detectability of agricultural signals within the present analytical framework.

Forest cover, particularly Closed Forest, emerged as a statistically significant buffering influence on river condition, showing strong negative associations with turbidity and TSS ($F = 10.30$, $p < 0.001$). Even within a landscape undergoing rapid extraction transformation, areas retaining a higher canopy cover appear to moderate sediment delivery to the river network. This finding is consistent with extensive evidence that forested riparian zones reduce overland flow velocities, improve infiltration, and trap sediments before they reach stream channels, thereby stabilising water quality downstream (Naiman and Decamps, 1997; Dosskey et al., 2010). The persistence of this buffering effect in the Ankobra basin underscores the disproportionate functional importance of remaining forest patches and riparian vegetation in extractive landscapes, where marginal changes in land cover can yield non-linear responses in river condition.

Settlements exhibited weaker but statistically significant associations with electrical conductivity (EC) and total dissolved solids (TDS), suggesting more subtle influences on river chemistry. EC values increased from approximately 65 $\mu S\ cm^{-1}$ in the upstream sections to over 12,000 $\mu S\ cm^{-1}$ near the estuary, while TDS concentrations exceeded 6000 $mg\ L^{-1}$ in downstream reaches. While part of this longitudinal gradient likely reflects estuarine processes and saline intrusion as the river approaches the coast, urban and infrastructural contributions — such as wastewater discharge, runoff from impervious surfaces, and altered hydrological pathways — may also play a role, particularly where sanitation infrastructure is limited (Paul and Meyer, 2001; Walsh et al., 2005). The co-occurrence of settlement expansion and elevated dissolved constituents highlights the need for caution when attributing chemical degradation to single land-use drivers and reinforces the importance of multivariate approaches capable of disentangling overlapping pressures. Given the modest sample size relative to the number of explanatory variables, these findings should be interpreted as indicative of spatial association rather than as definitive parameter estimates.

4.2. Implications for sustainability monitoring and management in extractive river basins

The results demonstrate that river degradation in the Ankobra basin is neither spatially uniform nor driven by an undifferentiated set of land-use pressures. Instead, sediment-related degradation is strongly concentrated in areas affected by mining-related disturbance, while other land uses exert weaker, more parameter-specific, or scale-dependent influences. This challenges conventional basin-wide monitoring approaches that assume homogeneous pressure and suggests that sustainability assessments would benefit from more spatially targeted and diagnostically informed strategies.

From a monitoring perspective, the dominance of mining-related land cover in explaining turbidity and total suspended solids indicates that surveillance and sampling effort should be prioritised along mining corridors and downstream reaches where disturbance is most intense. Uniform sampling designs that distribute limited resources evenly across a basin risk underrepresenting zones of acute impact while over-sampling relatively stable areas. An attribution-oriented framework allows monitoring programmes to be explicitly aligned with dominant pressures, improving both efficiency and interpretability. In contexts such as southern Ghana, where regulatory agencies often face constraints in personnel, funding, and analytical capacity, this prioritisation is important to maintain credible environmental oversight (Bebbington et al., 2018).

The results also have direct implications for regulatory enforcement and mitigation strategies. The clear association between Bareland/Mining and extreme sediment loads suggests that sediment control should be a central focus of environmental regulation in the basin, rather than a concern among many. Measures such as the enforcement of buffer zones, containment of spoil material, rehabilitation of abandoned mining pits, and restriction of hydraulic connectivity between disturbed surfaces and river channels are likely to yield disproportionate benefits for water quality relative to more diffuse interventions (Sengupta, 2021). Importantly, the attribution analysis indicates that targeting mining-related disturbance does not imply neglecting other land uses, but rather sequencing interventions according to their demonstrated impact. Such prioritisation enhances regulatory legitimacy by linking enforcement actions to observable environmental outcomes rather than to broad or symbolic compliance requirements.

The statistically significant buffering effect of forest cover further highlights the role of landscape configuration in mediating extractive impacts. Even within a heavily disturbed basin, areas that retain Closed Forest are associated with lower sediment loads, underscoring the functional value of forested and riparian vegetation for sustaining water-quality regulation. This supports management approaches that integrate forest conservation and restoration into extractive governance frameworks, not as compensatory add-ons but as core components of impact mitigation. Protecting remaining forest patches, strengthening riparian buffers and preventing sequential degradation from forest to open forest to bare disturbance may be particularly effective in slowing or reversing sediment escalation where mining activity persists. Such measures align with broader evidence on nature-based solutions to protect water-quality in disturbed basins (Dosskey et al., 2010).

At a broader governance level, the study illustrates how an attribution-oriented sustainability assessment can strengthen decision-making by clarifying responsibility and reducing ambiguity around environmental degradation. In many extractive contexts, environmental decline is widely recognised but contested in terms of causation, enabling blame shifting among sectors and undermining accountability. Empirically, distinguishing the relative contributions of different land-use pressures as demonstrated in this study provides a more transparent basis for regulatory prioritisation and stakeholder engagement. This is particularly relevant in settings characterised by overlapping formal and informal governance arrangements, where credibility and evidence-based justification are essential for effective intervention (Scoones, 2016; Newell, 2019).

Finally, while the findings are grounded in a specific basin, the implications extend beyond the Ankobra context. Many mineralised river basins in the Global South exhibit similar trajectories of forest loss, mining expansion, and fragmented monitoring regimes (e.g., Obodai et al., 2019; Asner et al., 2013; Diringer et al., 2020). The results suggest that sustainability outcomes in such systems depend less on the mere presence of extractive activity than on how land-use transitions unfold, where disturbance is concentrated, and whether residual buffering capacity is maintained.

5. Conclusion

This study links multi-decadal land-cover change with spatially modelled water-quality data to examine how contemporary extractive land-use pressures explain spatial variation in river condition within the Ankobra Basin. The results show that mining-related land disturbance is strongly associated with elevated turbidity and total suspended solids, while forest cover exhibits a contrasting buffering influence on sediment-related parameters. Agriculture and settlement showed weaker and more context-dependent relationships with the physico-chemical parameters examined. These findings indicate that water-quality degradation in extractive basins reflects the intensity

Table A.1
LULC transition matrices for the Ankobra River basin (km^2).

Transitions to 2002						
From/To	Water	Bareland/Mining	Settlement	Closed Forest	Open Forest	Agriculture
Water	3.45	0.01	0.14	4.75	4.26	0.57
Bareland/Mining	0.01	0.02	0.23	0.17	3.69	0.85
Settlement	0.10	0.16	5.10	1.18	11.26	3.59
Closed Forest	13.60	0.15	0.93	750.85	173.22	9.99
Open Forest	2.57	1.81	12.11	290.72	924.04	138.64
Agriculture	0.27	0.93	9.70	44.39	365.87	112.69
Transitions to 2016						
From/To	Water	Bareland/Mining	Settlement	Closed Forest	Open Forest	Agriculture
Water	3.47	0.85	1.10	6.66	5.66	1.70
Bareland/Mining	1.03	1.27	2.16	10.17	12.58	5.52
Settlement	0.50	1.68	11.76	22.56	72.64	37.78
Closed Forest	3.51	0.76	3.43	487.91	319.56	88.92
Open Forest	3.47	0.25	1.64	262.21	598.80	246.82
Agriculture	1.20	0.15	1.30	159.24	360.64	153.11
Transitions to 2025						
From/To	Water	Bareland/Mining	Settlement	Closed Forest	Open Forest	Agriculture
Water	4.64	1.54	0.89	1.71	1.42	0.63
Bareland/Mining	6.23	11.58	21.65	19.93	30.77	18.36
Settlement	0.93	4.47	36.95	24.35	47.97	33.98
Closed Forest	6.23	7.54	29.82	390.09	325.08	174.96
Open Forest	1.24	4.61	32.92	371.47	503.83	277.69
Agriculture	0.43	1.70	24.86	97.15	204.77	170.40

Values represent area transitions between LULC classes (km^2). Rows indicate source classes and columns indicate destination classes for each time period.

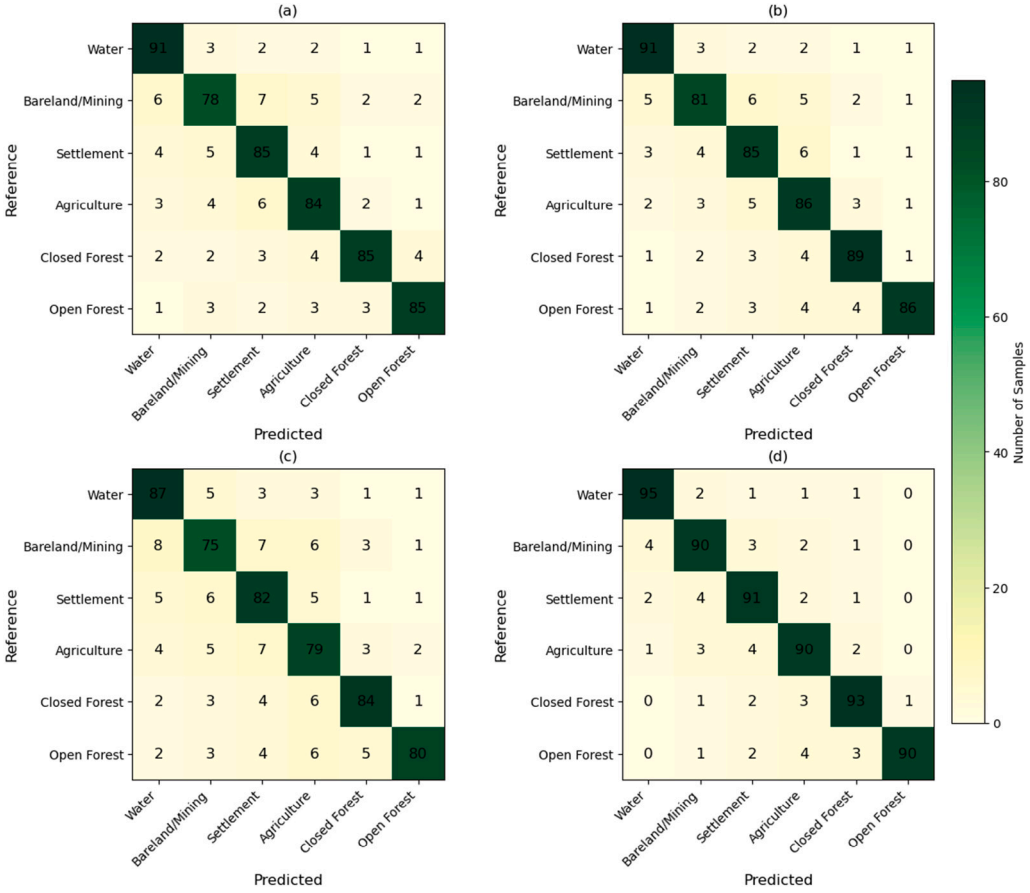

Fig. A.1. Confusion matrices for LULC classifications for (a) 1986, (b) 2002, (c) 2016, and (d) 2025. Rows represent reference classes and columns represent predicted classes. Cell values indicate the number of validation samples per class.

Table A.2
Area-adjusted land-cover estimates and corresponding percentage share of the total basin area, with 95% confidence intervals, for each land-cover class across the study periods.

Class	1986		2002		2016		2025	
	Area (km^2 ± CI)	Share (% ± CI)	Area (km^2 ± CI)	Share (% ± CI)	Area (km^2 ± CI)	Share (% ± CI)	Area (km^2 ± CI)	Share (% ± CI)
Water	84.66 ± 54.94	2.93 ± 1.90	50.89 ± 38.74	1.76 ± 1.34	98.96 ± 50.29	3.42 ± 1.74	26.97 ± 19.10	0.93 ± 0.66
Bareland/Mining	85.97 ± 59.16	2.97 ± 2.05	71.81 ± 51.33	2.48 ± 1.77	131.58 ± 58.70	4.55 ± 2.03	148.22 ± 41.01	5.13 ± 1.42
Settlement	140.08 ± 71.42	4.84 ± 2.47	123.29 ± 63.73	4.26 ± 2.20	258.11 ± 68.38	8.93 ± 2.36	209.52 ± 51.23	7.25 ± 1.77
Closed Forest	986.55 ± 97.39	34.11 ± 3.37	893.86 ± 85.75	30.91 ± 2.97	831.72 ± 94.53	28.76 ± 3.27	900.56 ± 70.65	31.14 ± 2.44
Open Forest	1290.61 ± 108.37	44.63 ± 3.75	1269.46 ± 92.11	43.90 ± 3.19	999.37 ± 90.37	34.56 ± 3.12	1145.53 ± 67.11	39.61 ± 2.32
Agriculture	304.15 ± 63.24	10.52 ± 2.19	482.70 ± 48.73	16.69 ± 1.68	572.07 ± 62.50	19.78 ± 2.16	461.14 ± 37.45	15.95 ± 1.29

Area-adjusted estimates were derived using accuracy-adjusted area estimation methods to account for classification uncertainty. Confidence intervals represent 95% uncertainty bounds around each estimate.

and spatial configuration of specific land-use pressures rather than a uniform landscape change. By explicitly linking land-use composition with observed water-quality variation, the framework provides diagnostic evidence that can support spatially targeted environmental management.

The analysis is based on cross-sectional dry-season sampling and near-stream land-use buffers and therefore does not capture seasonal variability, upstream hydrological connectivity, or historical water-quality trends associated with earlier phases of mining expansion. Extensions of this framework could therefore incorporate seasonal sampling, multi-scale buffer evaluation, river-network geostatistical approaches, upstream catchment metrics, or complementary process-based modelling to support more robust causal assessment. In particular, integrating historical land-cover change trajectories (e.g., mining expansion during 1986–2002 and 2002–2016) as explicit predictors of contemporary water-quality conditions would strengthen the evaluation of potential legacy sediment effects, provided that temporally aligned water-quality datasets are available. Integration of trace metal analysis (e.g. mercury, arsenic, and lead) alongside sediment indicators would further enable the assessment of both particulate and dissolved contamination pathways associated with gold mining in tropical river systems. Nonetheless, the approach demonstrated here provides a scalable and replicable means of linking land-use change to environmental outcomes in extractive landscapes, prioritising attribution, relevance, and decision support over methodological novelty alone.

CRediT authorship contribution statement

Vincent Adjei: Writing – original draft, Validation, Project administration, Methodology, Investigation, Formal analysis, Data curation, Conceptualization. **Lawson Mensah:** Writing – review & editing, Supervision, Conceptualization. **Alex Owusu Amoakoh:** Writing – review & editing, Writing – original draft, Supervision, Methodology, Conceptualization. **Mary Antwi:** Writing – review & editing, Supervision, Methodology, Conceptualization. **Gideon Nkrumah:** Writing – review & editing, Data curation. **Isaac Stanisluv Essah:** Writing – review & editing, Software, Methodology. **Frederick Gyan:** Writing – review & editing, Software, Data curation. **Vera Aseye Edor:** Writing – review & editing, Formal analysis, Data curation. **Godfred Adu Boateng:** Writing – review & editing, Methodology, Data curation.

Declaration of competing interest

The authors declare that they have no known competing financial interests or personal relationships that could have appeared to influence the work reported in this paper.

Appendix. LULC transition matrices

Appendix Table A.1 presents the LULC transition matrices for the Ankobra River basin, showing area-based transitions (km^2) between LULC classes for the periods 1986–2002, 2002–2016, and 2016–2025. The matrices provide detailed quantitative support for the dominant transition pathways discussed in the Results section and underpin the long-term land-use change patterns illustrated in Fig. 3.

Supplementary accuracy assessment outputs

This appendix provides supplementary materials supporting the LULC classification and change analysis presented in the main text. Fig. A.1 presents the full confusion matrices for each classification year (1986, 2002, 2016, and 2025), illustrating class-level agreement between reference data and model predictions. These matrices underpin the summary accuracy metrics reported in Section 3.2 and Table 4 and are included here to ensure transparency in the classification performance assessment.

A.1. Accuracy-adjusted land-cover area estimates

To account for classification uncertainty and provide statistically robust estimates of land-cover extent, accuracy-adjusted area estimates were derived for each LULC class and study year following standard post-classification adjustment procedures. Table A.2 reports the adjusted area estimates and corresponding percentage share of the total basin area, together with 95% confidence intervals. These estimates complement the mapped area statistics presented in Table 3 by quantifying uncertainty associated with classification error and enabling more reliable comparison of land-cover change across time.

References

Adusei, Y.Y., Quaye-Ballard, J., Adjaottor, A.A., Mensah, A.A., 2021. Spatial prediction and mapping of water quality of Owabi reservoir from satellite imageries and machine learning models. Egypt. J. Remote. Sens. Space Sci. 24 (3), 825–833. http://dx.doi.org/10.1016/j.ejrs.2021.06.006.

Allan, J.D., 2004. Landscapes and riverscapes: the influence of land use on stream ecosystems. Annu. Rev. Ecol. Evol. Syst. 35 (1), 257–284.

Allan, J.D., Manning, N.F., Smith, S.D., Dickinson, C.E., Joseph, C.A., Pearsall, D.R., 2017. Ecosystem services of lake erie: Spatial distribution and concordance of multiple services. J. Gt. Lakes Res. 43 (4), 678–688. http://dx.doi.org/10.1016/j.jglr.2017.06.001.

Amoakoh, A.O., Aplin, P., Awuah, K.T., Delgado-Fernandez, I., Moses, C., Alonso, C.P., Kankam, S., Mensah, J.C., 2021. Testing the contribution of multi-source remote sensing features for random forest classification of the greater Amanzule tropical peatland. Sensors 21 (10), 3399. http://dx.doi.org/10.3390/s21103399.

Amoakoh, A.O., Aplin, P., Rodríguez-Veiga, P., Moses, C., Alonso, C.P., Cortés, J.A., Delgado-Fernandez, I., Kankam, S., Mensah, J.C., Nortey, D.D.N., 2024. Predictive modelling of land cover changes in the Greater Amanzule peatlands using multi-source remote sensing and machine learning techniques. Remote. Sens. 16 (21), 4013. http://dx.doi.org/10.3390/rs16214013.

Armah, F.A., Obiri, S., Yawson, D.O., Pappoe, A.N.M., Akoto, B., 2010. Mining and heavy metal pollution: Assessment of aquatic environments in Tarkwa (Ghana) using multivariate statistical analysis. J. Environ. Stat. 1 (4), 1–13.

Asner, G.P., Llactayo, W., Tupayachi, R., Luna, E.R., 2013. Elevated rates of gold mining in the amazon revealed through high-resolution monitoring. Proc. Natl. Acad. Sci. USA 110 (46), 18454–18459. http://dx.doi.org/10.1073/pnas.1318271110.

Bebbington, A., Abdulai, A.G., Humphreys Bebbington, D., Hinfelaar, M., Sanborn, C., 2018. Governing Extractive Industries: Politics, Histories, Ideas. Oxford University Press.

Belgiu, M., Drăguţ, L., 2016. Random forest in remote sensing: A review of applications and future directions. ISPRS J. Photogramm. Remote Sens. 114, 24–31. http://dx.doi.org/10.1016/j.isprsjprs.2016.01.011.

Cudjoe, K., Nyantakyi, E.K., Borkloe, J.K., Adjei, E.A., Siabi, E.K., Ackerson, N.O.B., Yeboah, S.I.I.K., Domfeh, M.K., Wezenamo, C.A., Owusu, M., et al., 2023. Assessing livelihood and environmental implications of artisanal and small-scale mining: a case of Akango mining, Nzema East Municipality, Western Region, Ghana. Environ. Dev. Sustain. 1–28. http://dx.doi.org/10.1007/s10668-023-04339-x.

Diringer, S.E., Berky, A.J., Marani, M., Ortiz, E.J., Karatum, O., Plata, D.L., Pan, W.K., Hsu-Kim, H., 2020. Deforestation due to artisanal and small-scale gold mining exacerbates soil and mercury mobilization in Madre de Dios, Peru. Environ. Sci. Technol. 54 (1), 286–296. http://dx.doi.org/10.1021/acs.est.9b06620.

Dosskey, M.G., Vidon, P., Gurwick, N.P., Allan, C.J., Duval, T.P., Lowrance, R., 2010. The role of riparian vegetation in protecting and improving chemical water quality in streams. JAWRA J. Am. Water Resour. Assoc. 46 (2), 261–277. http://dx.doi.org/10.1111/j.1752-1688.2010.00419.x.

Duncan, A.E., de Vries, N., Nyarko, K.B., 2018. Assessment of heavy metal pollution in the sediments of the River Pra and its tributaries. Water Air Soil Pollut. 229 (8), 272. http://dx.doi.org/10.1007/s11270-018-3899-6.

EPA, 2009. Advice Note No. 5: Turbidity in Drinking Water. Environmental Protection Agency, Wexford, Ireland, URL: https://www.epa.ie/publications/compliance–enforcement/drinking-water/advice–guidance/Advice-Note-No5.pdf. Version 1, Issued 2 November 2009.

Foley, J.A., DeFries, R., Asner, G.P., Barford, C., Bonan, G., Carpenter, S.R., Chapin, F.S., Coe, M.T., Daily, G.C., Gibbs, H.K., et al., 2005. Global consequences of land use. Science 309 (5734), 570–574. http://dx.doi.org/10.1126/science.1111772.

Franklin, P., Stoffels, R., Clapcott, J., Booker, D., Wagenhoff, A., Hickey, C., 2019. Deriving Potential Fine Sediment Attribute Thresholds for the National Objectives Framework. National Institute of Water and Atmospheric Research Ltd, Hamilton, New Zealand, URL: https://environment.govt.nz/assets/Publications/Files/deriving-potential-fine-sediment-attribute-thresholds-for-the-national-objectives-framework.pdf.

Ghana Standards Authority, 2021. Water Quality – Specification for Drinking Water. Ghana Standards Authority, Accra, Ghana, URL: https://www.gsa.gov.gh/wp-content/uploads/2021/03/DGS-175_2021.pdf.

Gorelick, N., Hancher, M., Dixon, M., Ilyushchenko, S., Thau, D., Moore, R., 2017. Google earth engine: Planetary-scale geospatial analysis for everyone. Remote Sens. Environ. 202, 18–27. http://dx.doi.org/10.1016/j.rse.2017.06.031.

Hilson, G., 2002. The environmental impact of small-scale gold mining in Ghana: identifying problems and possible solutions. Geogr. J. 168 (1), 57–72. http://dx.doi.org/10.1111/1475-4959.00038.

Hilson, G., Sauerwein, T., Owen, J., 2020. Large and artisanal scale mine development: The case for autonomous co-existence. World Dev. 130, 104919. http://dx.doi.org/10.1016/j.worlddev.2020.104919.

Hudson-Edwards, K.A., Jamieson, H.E., Lottermoser, B.G., 2011. Mine wastes: past, present, future. Elements 7 (6), 375–380. http://dx.doi.org/10.2113/gselements.7.6.375.

Isidore, F., Cleophas, F., Moh, P.Y., Bidin, K., 2019. A pristine water quality of repeatedly logged forest river in Kawag forest area, Ulu Segama Malua forest reserve, Sabah. Trans. Sci. Technol. 6 (1), 48–53.

Jensen, J.R., 2016. Introductory Digital Image Processing: A Remote Sensing Perspective, fourth ed. Pearson, Boston.

Kuma, J.S., Younger, P.L., 2004. Water quality trends in the Tarkwa gold-mining district, Ghana. Bull. Eng. Geol. Environ. 63 (2), 119–132. http://dx.doi.org/10.1007/s10064-004-0227-8.

Li, J., Heap, A.D., 2014. Spatial interpolation methods applied in the environmental sciences: A review. Environ. Model. Softw. 53, 173–189. http://dx.doi.org/10.1016/j.envsoft.2013.12.008.

Ma, C., Sun, W., Yang, Z., Wang, J., Zhou, L., 2025. Spatiotemporal variations in land use impacts on river water quality in a mountain-to-plain transitional basin in arid region of northern China. J. Contam. Hydrol. 271, 104542. http://dx.doi.org/10.1016/j.jconhyd.2025.104542.

Minerals Commission of Ghana, 2026. Ghana mining repository. https://ghana.revenuedev.org. (Accessed March 2026).

Naiman, R.J., Decamps, H., 1997. The ecology of interfaces: riparian zones. Annu. Rev. Ecol. Syst. 28 (1), 621–658. http://dx.doi.org/10.1146/annurev.ecolsys.28.1.621.

Newell, P., 2019. Trasformismo or transformation? The global political economy of energy transitions. Rev. Int. Political Econ. 26 (1), 25–48. http://dx.doi.org/10.1080/09692290.2018.1511448.

Njue, N., Gräf, J., Weeser, B., Rufino, M.C., Breuer, L., Jacobs, S.R., 2021. Monitoring of suspended sediments in a tropical forested landscape with citizen science. Front. Water 3, 656770. http://dx.doi.org/10.3389/frwa.2021.656770.

Obodai, J., Adjei, K.A., Odai, S.N., Lumor, M., 2019. Land use/land cover dynamics using landsat data in a gold mining basin-the Ankobra, Ghana. Remote. Sens. Appl.: Soc. Environ. 13, 247–256. http://dx.doi.org/10.1016/j.rsase.2018.10.007.

Opoku, M.E., Salkushu, W., Hammond, F., 2017. A hybrid image classification approach to monitoring LULC changes in the mining district of Prestea-Huni Valley, Ghana. J. Environ. Earth Sci. 7 (3), 1–10.

Osei, J.D., Arhin, E., Twumasi, Y.A., Yevugah, L.L., Boakye, L., Damoah-Afari, P., Saah, D., Coffie, P.B., 2024. Poisoned for gold: Assessing the spatial extent of heavy metal contamination within the Tutua-Bura-Angoben shelter belt forest reserve in Ghana. Watershed Ecol. Environ. 6, 146–154. http://dx.doi.org/10.1016/j.wsee.2024.08.001.

Paul, M.J., Meyer, J.L., 2001. Streams in the urban landscape. Annu. Rev. Ecol. Syst. 32 (1), 333–365. http://dx.doi.org/10.1146/annurev.ecolsys.32.081501.114040.

Scoones, I., 2016. The politics of sustainability and development. Annu. Rev. Environ. Resour. 41 (1), 293–319. http://dx.doi.org/10.1146/annurev-environ-110615-090039.

Sengupta, M., 2021. Environmental Impacts of Mining: Monitoring, Restoration, and Control. CRC Press, Boca Raton, FL.

Turnhout, E., Metze, T., Wyborn, C., Klenk, N., Louder, E., 2020. The politics of co-production: participation, power, and transformation. Curr. Opin. Environ. Sustain. 42, 15–21. http://dx.doi.org/10.1016/j.cosust.2019.11.009.

Walsh, C.J., Roy, A.H., Feminella, J.W., Cottingham, P.D., Groffman, P.M., Morgan, R.P., 2005. The urban stream syndrome: current knowledge and the search for a cure. JNABS 24 (3), 706–723. http://dx.doi.org/10.1899/04-028.1.

Wiafe, S., Awuah Yeboah, E., Boakye, E., Ofosu, S., 2022. Environmental risk assessment of heavy metals contamination in the catchment of small-scale mining enclave in Prestea Huni-Valley District, Ghana. Sustain. Environ. 8 (1), 2062825. http://dx.doi.org/10.1080/27658511.2022.2062825.

World Health Organization, 2017. Guidelines for Drinking-water Quality, fourth ed. World Health Organization, Geneva, URL: https://www.who.int/publications/i/item/9789241549950.